



## Studies on the Ion Exchange Properties of Modified and Unmodified Orange Mesocarp Extract in Aqueous Solution

Millicent U. Ibezim-Ezeani\*, Francis A. Okoye and Onyewuchi Akaranta

Department of Pure and Industrial Chemistry, University of Port Harcourt, P.M.B. 5323, Choba, Port Harcourt, Nigeria

\*E-mail: millibejmj@yahoo.com

### ABSTRACT

*This investigation describes the ion exchange properties of orange mesocarp extract (OME), Carboxylated-Toluene Di-isocyanate Orange Mesocarp Extract Resin (CTOR) and Sulphonated-Toluene Di-isocyanate Orange Mesocarp Extract Resin (STOR) for the removal of metal ions in aqueous solution. The Infrared absorption bands of OME, CTOR and STOR indicate the presence of possible functional groups that may enhance ion exchange reaction. The effect of varying initial metal ion concentration on the ion exchange process was studied at 29°C. It was found that the uptake of Zn<sup>2+</sup>, Cu<sup>2+</sup>, Ni<sup>2+</sup> and Co<sup>2+</sup> ions by OME, CTOR and STOR is related to the dissociation power of the exchangeable hydrogen and in sequence similar to the ionic radii of the metal ions. The Dubinin-Radushkevich (D.R.) isotherm parameters revealed that the uptake of metal ion by OME proceeded by physical adsorption ( $E = 0.1581$  kJ/mol), while the uptake of metal ion by CTOR and STOR proceeded by ion exchange mechanism ( $E = 8.452 - 11.180$  kJ/mol).*

**KEYWORDS:** Orange mesocarp, Ion exchange, Heavy metals, Resin, Effluent treatment.

### INTRODUCTION

Ion exchange and its principles have wide applications in analytical chemistry, hydrometallurgy, antibiotic purification, separation of radioisotopes, water treatment, and pollution control [1]. Ion exchange removes unwanted ions from solution by transferring them to a solid material (ion exchanger) which accepts them while giving back an equivalent number of desirable species stored on the ion exchange skeleton [2]. According to Jorgensen and Weatherley, the traditional method for removal of ammonium and organic pollutants from wastewater is biological treatment, but ion exchange offers a number of advantages including the ability to handle shock loadings and operate over a wider range of temperatures. The experimental results show that in most of the cases studied, the presence of organic compounds enhanced the uptake of ammonium ion onto the ion exchanger [3]. The quality of surrounding, fresh and marine water varies directly with the healthy growth, propagation and harvests of both plants and animals. A large quantity of sewage, industrial effluents and domestic waste are discharged daily. These consist of various hazardous chemicals consequently causing deleterious effects on the environment and aquatic life. Among these pollutants are heavy metals such as Cu, Mn, Mo, Ni, V, Zn, Co, Pb, Hg, Cd, Cr and F, which are not subject to nutritive bacterial attack or other biological break down and are permanent additions to environment, rivers, sediments and atmosphere. The conventional treatment techniques like precipitation, oxidation / reduction, complexation, adsorption and ion exchange are expensive, not eco-friendly and has the disadvantage of sludge production. Amongst these techniques, only adsorption and ion exchange are considered as the option for remediation with least ecological problem. However, chemical adsorbents and ion exchange resins are expensive and the increasing demand of eco-friendly technologies has led to the search of low-cost alternatives with ease of maintenance and regeneration. Mesocarp from orange fruit is the raw material utilized in this research and has also been applied in other investigations. It contains polyhydroxy-phenols which can bind metal by ion exchange mechanism and is used for animal and fish feed, accelerating compost and fermentation, aeration of clay soil and food flavouring. Akaranta and Osuji formulated drilling mud from orange mesocarp cellulose with carboxymethylation to a degree of substitution of 0.45 – 0.63. The results showed that the drilling mud formulated with orange mesocarp- based sodium carboxymethyl cellulose has physical properties comparable to drilling mud formulated with a commercial sodium carboxymethyl cellulose [4].

Results from the removal of some metal ions from aqueous solution by Ogali *et al.* showed that unmodified orange mesocarp residue after extraction of rutin bound 56% of Mg, 81% of Zn, 71% of Cu, 73% of Pb and 85.05% of Cd, while the modified form was able to bind 63.05% of Mg, 37% of Zn, 43.25% of Cu, 33.05% of Pb and 86.45% of Cd [5]. Oranges are taken daily in this part of the world and utilized in large quantities by fruit juice and wine production industries. The need therefore arises to harness the residue for gainful use in order to reduce the polluting effects that the dumping of millions of tones orange waste would impact on the environment. Hence, the objective of this study is to develop and examine the properties of a contemporary economically feasible and environmental friendly ion exchange resin from orange mesocarp extract for the removal of metal ions from aqueous solutions and industrial effluents.

## MATERIALS AND METHODS

### Collection and Preparation of Orange Mesocarp Sample

Fresh oranges bought from Choba market in River State, Nigeria was utilized for this study. The epicarp was thoroughly peeled off, the mesocarp carefully removed from the juicy part and sun dried for eight days. The dried orange mesocarp was ground with a hand grinding mill, sieved to obtain 106 $\mu$ m particle size and stored in a plastic container at ambient atmospheric condition.

### Extraction of Rutin

Rutin was extracted from 2810g of 106 $\mu$ m size orange mesocarp with soxhlet extractor using methanol as extracting solvent. The methanol-extract mixture was evaporated using rotor evaporator to expel the remaining methanol from the extract sample.

### Synthesis of the Resin

In a 1L beaker containing 53g of 4-Hydroxybenzoic acid dissolved in 226ml of acetone (or 40ml Phenoxy-4-sulphonic acid in 90ml of acetone), 400ml toluene diisocyanate (TDI) was added and stirred vigorously. 80g of extract in 250ml of methanol was poured into the mixture with continuous stirring, the resultant product was a brown solid. The resin formed was left overnight before use. This was then crushed, sieved to different sizes and stored in tightly covered bottles at room temperature (29°C).

### Preparation of Metal Ion Stock Solutions

4.397g of Zn<sup>2+</sup> (ZnSO<sub>4</sub>.7H<sub>2</sub>O), 3.803g of Cu<sup>2+</sup> [Cu(NO<sub>3</sub>)<sub>2</sub>.3H<sub>2</sub>O], 4.460g of Ni<sup>2+</sup> (NiSO<sub>4</sub>.6H<sub>2</sub>O) and 4.770g of Co<sup>2+</sup> (CoSO<sub>4</sub>.7H<sub>2</sub>O) were each dissolved in 1.0L of distilled deionised water to obtain 1000mg/L metal ion stock solution respectively. Serial dilution of the stock solutions was carried out to obtain working standards of 5 – 70mg/L solutions for Zn (II), Cu (II), Ni (II) and Co (II) ions.

### Fourier Transform Infrared Spectroscopic Studies

FTIR spectroscopy was used to identify the functional groups present in the OME, CTOR and STOR samples. 0.0035g OME / CTOR / STOR sample was mixed with 0.5g KBr and pressed to form pellet. The samples were examined using FTIR spectrometer (prestige 21 shimadzu corporations) within the range 400 – 4000cm<sup>-1</sup>.

### Ion Exchange Studies

1.0 gram of OME / CTOR / STOR sample was added to 50ml of 50mg/L metal (Zn<sup>2+</sup> / Cu<sup>2+</sup> / Ni<sup>2+</sup> / Co<sup>2+</sup>) ion solution in 150ml conical flask and corked. The flask was then shaken in a mechanical shaker (120 oscillations / min) for one hour at 29°C. After the shaking period, the solution was filtered through a glass wool and the concentration of metal ion (Zn<sup>2+</sup>, Cu<sup>2+</sup>, Ni<sup>2+</sup> and Co<sup>2+</sup>) in the filtrate analysed using the Buck Scientific Atomic Absorption Spectrophotometer (model 205 A). The above experiment was repeated at different concentrations of 5 to 70mg/L. The ion exchange capacity (q<sub>e</sub>) in mg/g was determined using the mass balance equation expressed as equation (1) and plotted as a function of initial metal ion concentration.

$$q_e = \frac{V}{m} (C_o - C_e) \quad (1)$$

where C<sub>o</sub> is the initial metal ion concentration in solution (mg/L) and C<sub>e</sub> is the metal ion concentration in solution (mg/L) at equilibrium, V is volume of initial metal ion solution used (L), and m is mass of OME / CTOR / STOR used (g).

In order to distinguish the mechanism involved in the uptake of metal ion by the OME, CTOR and STOR, the values of ion exchange capacity were tested with Dubinin-Radushkevich isotherm model,

which is based on the Polanyi theory [6,7]. The linear form of Dubinin-Radushkevich (D.R.) equation is expressed as:

$$\ln q_e = \ln q_D - B_D \left[ RT \ln \left( 1 + 1/C_e \right) \right]^2 \quad (2)$$

where  $q_D$  is the maximum ion exchange capacity,  $[RT \ln (1 + 1/C_e)]$  is equal to the Polanyi potential,  $R$  is gas constant,  $T$  is temperature (29°C),  $B_D$  is related to the mean free energy of sorption per mole of the metal ion as it migrates to the surface of the ion exchanger from infinite distance in the solution and this energy can be evaluated using the relationship [8]:

$$E = \frac{1}{\sqrt{2B_D}} \quad (3)$$

If the magnitude of  $E$  is between 8 and 16 kJ/mol, the sorption process proceeds by ion exchange, while the sorption process is physical in nature if the value of  $E < 8$  kJ/mol.

## RESULTS AND DISCUSSION

### Spectroscopic Analysis

Figures 1, 2 and 3 show the infrared spectra of OME, CTOR and STOR respectively at the percentage transmittance for various wave numbers. Infrared absorption bands and their possible group assignments are presented in Table 1.

The infrared spectrum of OME (Figure 1) showed a sharp absorption band at 3279.02  $\text{cm}^{-1}$  due to free OH stretching and absorption band at 1560 - 1500  $\text{cm}^{-1}$  due to C=C stretching of aromatic ring vibration [9]. A weak peak at 1405  $\text{cm}^{-1}$  may be ascribed to the carboxylate ion giving rise to a weak symmetrical stretching band near 1400  $\text{cm}^{-1}$  [10]. The sharp peaks at 1300  $\text{cm}^{-1}$  and 1129.88  $\text{cm}^{-1}$  indicate the presence of C-O stretching of alcohols, phenols and ethers, while the absorption bands at 845.52, 833.01 and 700.94  $\text{cm}^{-1}$  reveal an out-of-plane deformation mode of C-H in various substituted benzene rings [11]. The absorption bands at 626.02 and 568.57  $\text{cm}^{-1}$  could be associated with the powdered potassium bromide used in sample preparation for infrared analysis, since brominated compounds absorb in the 690 – 515  $\text{cm}^{-1}$  region [10].

The infrared spectrum of CTOR (Figure 2) exhibits a broad band at 3440 – 3270  $\text{cm}^{-1}$  with a maximum at 3290.41  $\text{cm}^{-1}$  which is attributed to the asymmetric and symmetric hydroxyl –OH stretches [12]. This band at 3290.41 also suggests the presence of N-H stretching [9]. The sharp peak at 2930.67  $\text{cm}^{-1}$  is in the C-H stretching region of 3000 – 2800  $\text{cm}^{-1}$  [13]. A very small peak at 1710 – 1680  $\text{cm}^{-1}$  is assigned to C=O stretching of unsaturated carboxylic acid, while the absorption peak at 1641.75  $\text{cm}^{-1}$  is assigned to C=N stretching. The spectrum also showed strong absorption bands at 1598.02 and 1503.40  $\text{cm}^{-1}$  due to aromatic ring C=C stretching vibrations enhanced by polar functional groups [9]. The absorption peak at 1429.30  $\text{cm}^{-1}$  indicates the presence of carboxylate ion giving rise to a weak symmetrical stretching band near 1400  $\text{cm}^{-1}$  [10], while the peak at 1350.04  $\text{cm}^{-1}$  is in the C-O stretching region of 1350 – 1250  $\text{cm}^{-1}$ . Small absorption peaks between 1208.28 and 1012.44  $\text{cm}^{-1}$  suggest the presence of C-O stretching of alcohols, carboxylic acids and ethers, while the absorption peaks at 845.38, 830.46 and 700.83  $\text{cm}^{-1}$  indicate C-H stretching of mono- and disubstitutions on the benzene ring [9]. The absorption bands at 625.88 and 568.56  $\text{cm}^{-1}$  could be associated with the powdered potassium bromide used in sample preparation for infrared analysis, since brominated compounds absorb in the 690 – 515  $\text{cm}^{-1}$  region [10].

The infrared spectrum of STOR (Figure 3) shows a wide absorption band at 3530 – 3220  $\text{cm}^{-1}$  with a maximum at 3316.13  $\text{cm}^{-1}$  which could be assigned to the O-H stretching mode of hydroxyl groups [13] and N-H stretching [9]. The absorption band at 1655  $\text{cm}^{-1}$  indicates the presence of C=N stretching, while the bands at 1592.45 and 1502.44  $\text{cm}^{-1}$  indicate the presence of aromatic ring C=C stretching vibrations enhanced by polar functional groups [9]. The absorption peak at 1431.39  $\text{cm}^{-1}$  indicates the presence of carboxylate ion giving rise to a weak symmetrical stretching band near 1400  $\text{cm}^{-1}$  [10]. Absorption bands at 1163.83 and 1032.79  $\text{cm}^{-1}$  could be assigned to C-O stretching of alcohols, phenols and ethers, also, sulphur compounds such as sulphonic bridges may contribute to absorption between 1300 – 1000  $\text{cm}^{-1}$  as well [11]. Silverstein *et al.* reported S=O stretching of sulphonic acid at 1165 – 1150  $\text{cm}^{-1}$  [10]. The absorption bands at 834.04 and 701.45  $\text{cm}^{-1}$  could be assigned to the characteristic absorption of polynuclear aromatics resulting from C-H out of plane bending in the 900 – 675  $\text{cm}^{-1}$  region whereas the band at 571.32  $\text{cm}^{-1}$  could be associated with the powdered potassium

bromide used in sample preparation for infrared analysis, since brominated compounds absorb in the 690 – 515  $\text{cm}^{-1}$  region [10].

The most remarkable difference in the infrared spectra of OME, CTOR and STOR studied is with the percentage transmittance which is in the order: OME > CTOR > STOR, this trend could be explained based on the relative difference in band intensity corresponding to the difference in the concentration of the respective functional groups associated with the bands. The mechanism of CTOR and STOR coupling is shown in Figure 4.

**Table 1:** Infrared Absorption Bands and their Possible Group Assignments

Possible Group	Functional	Absorption Bands ( $\text{cm}^{-1}$ )		
		OME	CTOR	STOR
O-H stretching		3279.02	3290.41	3316.13
N-H stretching			3440 – 3270	3530 – 3220
C-H stretching			2390.67	
C=O stretching			1710 – 1680	
C=N stretching			1641.75	1655
C=C stretching		1560, 1500	1598.02, 1503.40	1592.45, 1502.44
O-C=O stretching		1405	1429.30	1431.39
C-O stretching		1300, 1208.46, 1177.69, 1129.88	1350.04, 1208.28, 1177.63, 1036.41, 1012.44	1163.83, 1032.79
S=O stretching				1163.83
C-H stretching		845.52, 833.01, 700.94	845.38, 830.46, 700.83	834.04, 701.45
Br stretching		626.02, 568.57	625.88, 568.56	571.32

**Table 2:** D.R. parameters

D.R. parameters	OME				CTOR				STOR			
	Zn <sup>2+</sup>	Cu <sup>2+</sup>	Ni <sup>2+</sup>	Co <sup>2+</sup>	Zn <sup>2+</sup>	Cu <sup>2+</sup>	Ni <sup>2+</sup>	Co <sup>2+</sup>	Zn <sup>2+</sup>	Cu <sup>2+</sup>	Ni <sup>2+</sup>	Co <sup>2+</sup>
q <sub>D</sub> (mg/g)	0.049	0.042	0.031	0.024	1.508	1.703	1.775	1.971	1.919	2.136	2.229	2.364
B <sub>D</sub> (mol <sup>2</sup> /J <sup>2</sup> )	2E-05	2E-05	2E-05	2E-05	6E-09	5E-09	5E-09	4E-09	7E-09	6E-09	5E-09	4E-09
E(kJ/mol)	0.158	0.158	0.158	0.158	9.129	10.000	10.000	11.180	8.451	9.129	10.000	11.180
R <sup>2</sup>	0.9986	0.9973	0.9992	0.9995	0.9996	0.9997	0.9996	0.9994	0.9995	0.9995	0.9995	0.9995

### Effect of Concentration

The effect of varying initial metal ion concentration on the ion exchange reaction at 29°C is represented in Figure 5.

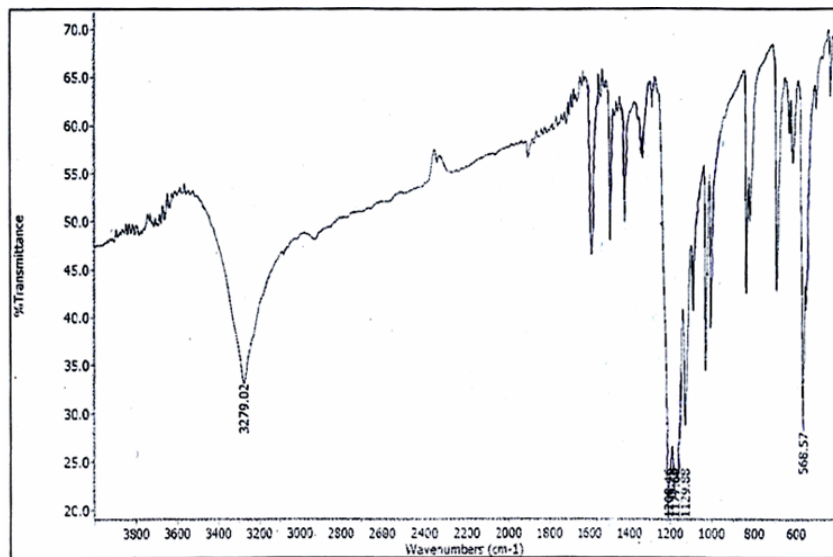


Fig. 1: Infrared Spectrum of OME

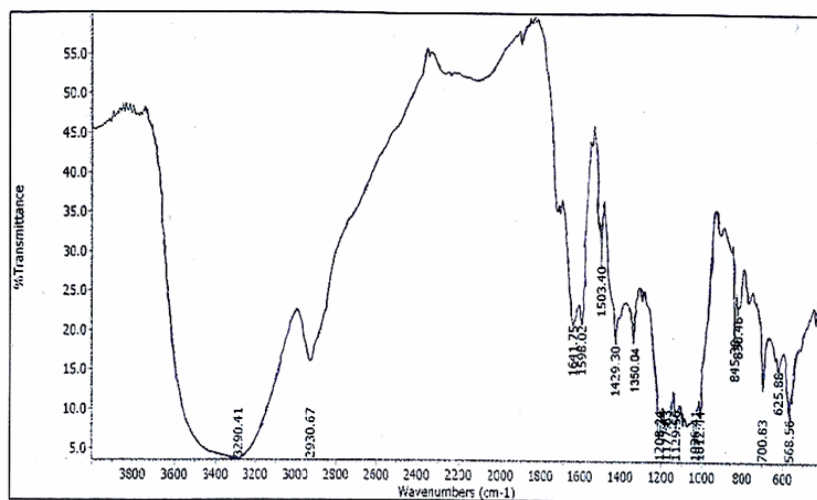


Fig. 2: Infrared Spectrum of CTOR

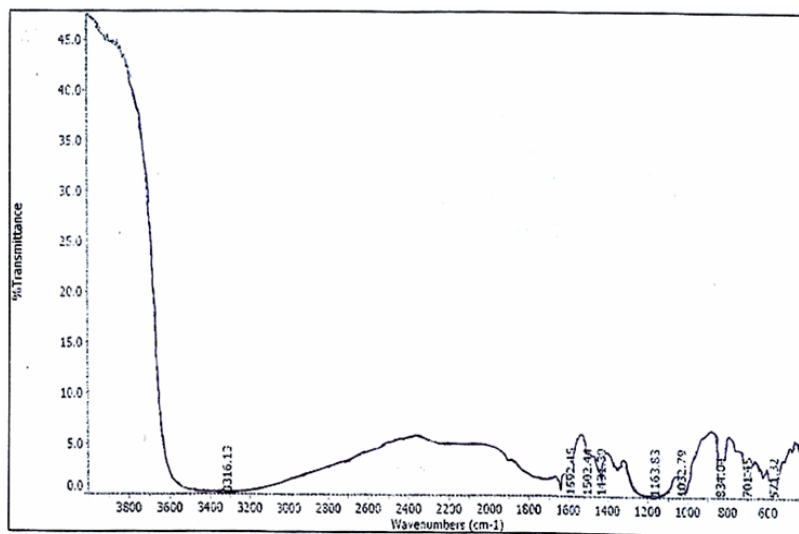


Fig. 3: Infrared Spectrum of STOR

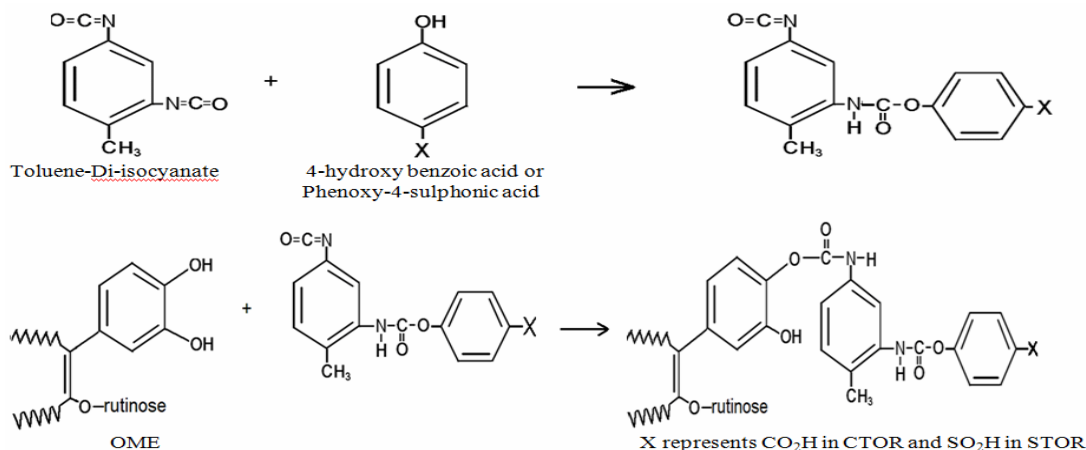
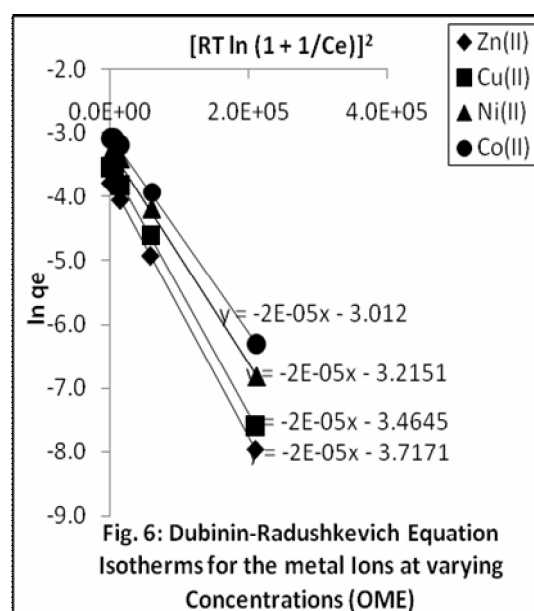
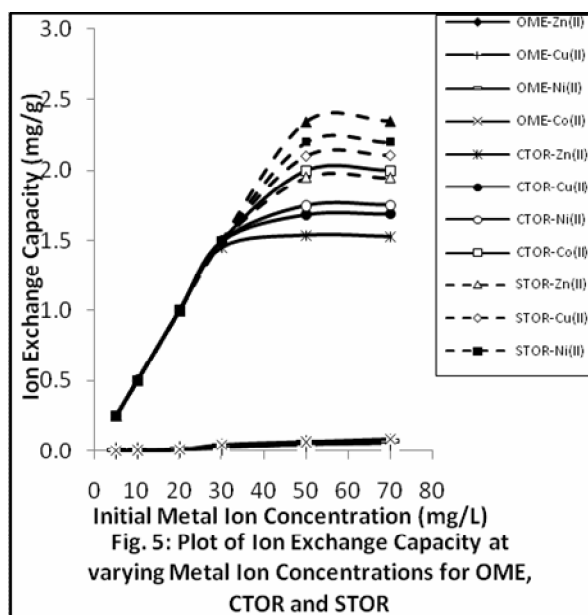
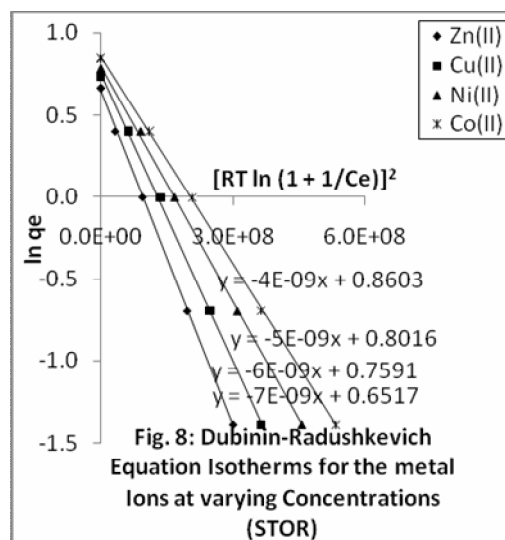
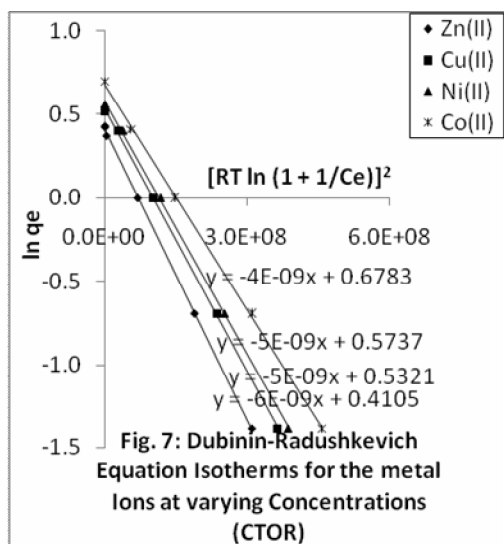


Fig. 4: Mechanism of CTOR and STOR coupling



It is evident from Figure 5 that the rate of ion exchange is a function of the initial metal ion concentration. The ion exchange capacity of the OME, CTOR and STOR increased with increase in the initial concentrations of Zn<sup>2+</sup>, Cu<sup>2+</sup>, Ni<sup>2+</sup> and Co<sup>2+</sup> ions and reaching a maximum at 30mg/L for OME, 50mg/L for CTOR and 50mg/L for STOR. It could be that at lower initial concentration, the fewer metal ions present in solution interact with the available exchange sites, thereby facilitating the ion exchange. As initial metal ion concentration increases from 5 to 30mg/L, and with available exchange sites remaining constant, the ion exchange capacity increased rapidly due to the presence of more metal ions in solution to compete for the fixed number of binding sites on the exchanger until a maximum ion exchange limit is attained which signifies the saturation of the active sites with some metal ions left unexchanged in solution. In all the experiments, the ion exchange capacity was found to be in the order: STOR > CTOR > OME. This trend could be associated with the dissociation power of the hydrogen in the main ionogenic functional group of the exchanger in aqueous solution which is -OH for OME, -CO<sub>2</sub>H for CTOR and -SO<sub>3</sub>H for STOR. Following the Bronsted-Lowry theory which states that an acid is a substance that is capable of donating a proton, OME, CTOR and STOR could be classified as acids since they are characterized by the functional groups: -OH, -CO<sub>2</sub>H and -SO<sub>3</sub>H respectively which bear proton that can dissociate in solution. It is the ease with which the bond



holding the proton (exchangeable hydrogen) to the structure of the species are broken that determines the strength of the acid and hence its ability to be displaced by metal ion. An observation of the active sites of OME, CTOR and STOR (Figure 4) shows that the tendency of the proton to dissociate is influenced by the attachment of more electron withdrawing atoms to the C, C and S of the OME, CTOR and STOR sites respectively. There are two O atoms attached to S in STOR which are not bonded to any other atom while in CTOR, there is only one O atom attached to C. The S atom in STOR exchanger experiences the electron withdrawing ability of two oxygen atoms while the C atom in CTOR experiences the electron withdrawing ability of one oxygen atom. The depletion of electron density around the S atom in STOR is therefore twice the depletion of electron density around the C atom in CTOR, hence the greater tendency of the proton to dissociate in STOR and its greater acid strength<sup>[14]</sup>. In the case of OME, there is no O or electron withdrawing atom attached to the C atom to facilitate the ease of breaking of the O-H bond and this explains the very low ion exchange capacity of OME.

From the above discussion, the order of the ease of proton dissociation is STOR > CTOR > OME, which is in line with the observed order of their ion exchange capacities, confirming that STOR exhibited greater ability for exchange reaction.

In terms of the metal ion exchange, the ion exchange capacity is in the order:  $\text{Co}^{2+} > \text{Ni}^{2+} > \text{Cu}^{2+} > \text{Zn}^{2+}$ . The order is similar to the order of the ionic radii ( $\text{Zn}^{2+} = 0.74\text{\AA}$ ,  $\text{Cu}^{2+} = 0.73\text{\AA}$ ,  $\text{Ni}^{2+} = 0.69\text{\AA}$  and  $\text{Co}^{2+} = 0.65\text{\AA}$ ) of the metal ions [15], suggesting that the smaller the size of the metal ion, the easier its diffusion to the exchange sites and hence, the higher the ion exchange capacity. In this case,  $\text{Co}^{2+}$  with the smallest radius and greatest access to the exchange sites exhibited the highest ion exchange capacity followed by  $\text{Ni}^{2+}$ ,  $\text{Cu}^{2+}$  and  $\text{Zn}^{2+}$  ions.

#### Dubinin-Radushkevich (D.R.) Isotherm

The plots of  $\ln q_e$  versus  $[\text{RT} \ln (1 + 1/C_e)]^2$  for the uptake of metal ion on the OME, CTOR and STOR are shown in Figures 6, 7 and 8 respectively. The parameters obtained in the D.R. equation are presented in Table 2.

The D.R. parameters calculated from the slope and intercept of the linear plots show that the values of E for the uptake of metal ion by the OME is less than 8 kJ/mol which is within the energy range of physical adsorption, while the values of E for the uptake of metal ion by the CTOR and STOR are in the order of an ion exchange mechanism, in which the sorption energy lies within 8 – 10 kJ/mol.

#### CONCLUSION

This investigation showed that the infrared spectroscopic results are in conformity with the proposed structure of OME, CTOR and STOR. The ion exchange capacity of OME, CTOR and STOR was found to be a function of the initial metal ion concentration. Experimental results revealed that the ion exchange capacity is in the order: STOR > CTOR > OME, which is in similar trend with their

dissociation strength. In terms of metal ion, the ion exchange capacity is in the order:  $\text{Co}^{2+} > \text{Ni}^{2+} > \text{Cu}^{2+} > \text{Zn}^{2+}$ , which corresponds to the order of the ionic radii of the metal ions. The sorption processes were described by D.R. isotherm model, with values of E indicating that the mechanism of metal interaction with OME is physical adsorption, while that with CTOR and STOR is of ion exchange mechanism. This study has demonstrated that CTOR and STOR exhibit good ion exchange capacity that may warrant their application in water / effluent treatment systems.

## REFERENCES

- [1] Vasudevan Padma and Sarma N.L.N. (1979). Composite Cation Exchange. *Journal of Applied Polymer Science*, **23**: 1443 – 1448.
- [2] Elshazly, A. H. and Konsowa, A. H. (2005). Removal of Nickel Ions from Wastewater Using a Cation-Exchange Resin in a Batch-Stirred Tank Reactor. *Desalination*, **158**: 189-193.
- [3] Jorgensen, T. C. and Weatherley, L. R. (2003). Ammonia Removal from Wastewaters by Ion Exchange in the Presence of Organic Contaminants. *Water Research*, **37**: 1723-1728.
- [4] Akaranta, O. and Osuji, L. C. (1997). Carboxymethylation of Orange Mesocarp Cellulose and its Utilization in Drilling Mud Formulation. *Cellulose Chemistry and Technology*, **31**: 193-198.
- [5] Ogali, R. E., Akaranta, O. and Aririguzo, V. O. (2008). Removal of Some Metal Ions from Aqueous Solution Using Orange Mesocarp. *African Journal of Biotechnology*, **7** (17): 3073-3076.
- [6] Erdem, E., Karapinar, N. and Donat, R. (2004). The Removal of Heavy Metal Cations by Natural Zeolites. *Journal of Colloid and Interface Science*, **280**: 309-314.
- [7] Mahramanlioglu, M., Kizilcikli, I. and Bicer, I. O. (2002). Adsorption of Fluoride from Aqueous Solution by Acid Treated Spent Bleaching Earth. *Journal of Fluoride Chemistry*, **115**: 41-47.
- [8] Ho, Y. S., Porter, J. F. and McKay, G. (2002). Equilibrium Isotherm Studies for the Sorption of Divalent Metal Ions onto Peat: Copper, Nickel and Lead Single Component Systems. *Water, Air, and Soil Pollution*, **141**: 1-33.
- [9] Uzoukwu, B. A. (2009). Basic Analytical Chemistry, Millennium edn., Paragraphics, Port Harcourt, Nigeria. pp. 275-281.
- [10] Silverstein, R. M., Bassier, G. C. and Morrill, T. C. (1991). Spectrometric Identification of Organic Compounds, 5th Edn., John Wiley and Sons, Inc. USA. pp. 91-102.
- [11] Puziy, A. M., Poddubnaya, O. I., Martínez-Alonso, A., Suárez-García, F. and Tascón, J.M.D. (2002). Synthetic Carbons Activated with Phosphoric Acid I. Surface Chemistry and Ion Binding Properties. *Carbon*, **40**: 1493-1505.
- [12] Jignasa, A., Thakkar, R. and Uma, C. (2006). A Study on Equilibrium and Kinetics of Ion Exchange of Alkaline Earth Metals Using an Inorganic Cation Exchanger – Zirconium Titanium Phosphate. *J. Chem. Science*, **118** (2): 185-189.
- [13] Shin, E. W., Karthikeyan, K. G. and Tshabalala, M. A. (2007). Adsorption Mechanism of Cadmium on Juniper Bark and Wood. *Bioresource Technology*, **98**: 588-594.
- [14] Anusiem, A. C. I. (2000). Principles of General Chemistry, Revised edn., Versatile Publishers, Owerri, Nigeria. p. 441.
- [15] Lee, J. D. (1996). Concise Inorganic Chemistry, 5th edn., Blackwell Science Ltd., New York. pp. 786-839.